Evaluation of Spectrodirectional Alfalfa Canopy Data Acquired During DAISEX'99

Gabriela Strub, Michael E. Schaepman, Yuri Knyazikhin, and Klaus I. Itten, *Senior Member, IEEE*

***Abstract*—Field goniometer measurements are a tool to generate *a priori* bidirectional reflectance distribution function (BRDF) knowledge for correction and validation of directional reflectance data acquired by air- and spaceborne sensors. This study analyzes the diurnal hemispherical-directional reflectance factor data of an Alfalfa canopy measured during the Digital Airborne Imaging Spectrometer Experiment 1999 (DAISEX'99). We analyze the variation of measured and modeled spectrodirectional vegetation data, revealing that measurement noise is negligible compared to the variation due to the canopy's anisotropy. The deviations of the spectral albedo (bihemispherical reflectance) and of field spectrometer nadir measurements throughout a day prove to be larger than modeled deviations. Calculated anisotropy factors quantify the spectral-dependent effects of the vegetation reflectance anisotropy. This paper is a contribution toward the generation of a reliable BRDF database by suggesting methods to preprocess and analyze observed directional vegetation reflectance data, with special emphasis on the spectral dimension.**

***Index Terms*—Alfalfa, bidirectional reflectance distribution function (BRDF), spectral bihemispherical reflectance (BHR), spectral hemispherical-directional reflectance factor (HDRF).**

I. Introduction

FIELD goniometer measurements are used to validate, calibrate, or correct bidirectional effects present in air- and spaceborne sensor data. Recent works show good agreement between directional ground-based and airborne imaging spectrometer hemispherical-directional reflectance factor (HDRF) and radiance data [1], [2]. Further, *a priori* knowledge of directional reflectance properties in the form of field measurements improve the retrieval of surface bidirectional reflectance and spectral albedo from satellite data [3]. Results of early field campaigns (e.g., Large Area Crop Inventory Experiment, known as LACIE) and Agriculture and Resources Inventory Surveys Through Aerospace Remote Sensing, known as AgRISTARS) already recognized the importance of spectrodirectional measurements [4]. Although such data of Alfalfa canopies were acquired in the past, the performed analysis focused on integrated broadband red and near-infrared (NIR) directional reflectances in order to determine the influence of the view and sun direction on vegetation indices [5], [6].

Manuscript received April 18, 2002; revised January 18, 2003. This work was supported by the Swiss National Science Foundation under Contract 2000-06431.00, by Astrium GmbH, and by the University of Valencia. The work of J. Moreno was supported under European Space Agency Contract 15343/01/NL/MM.

G. Strub, M. E. Schaepman, and K. I. Itten are with the Remote Sensing Laboratories, Department of Geography, University of Zürich, 8057 Zürich, Switzerland (e-mail: gstrub@geo.unizh.ch).

Y. Knyazikhin is with the Department of Geography, Boston University, Boston, MA 02215 USA.

Digital Object Identifier 10.1109/TGRS.2003.811555

This paper aims at the quantification of additional information contained in diurnal spectral HDRFs of an Alfalfa (*Medicago sativa*) canopy, in contrast to multispectral unidirectional reflectance data. Field Goniometer System (FIGOS) [7] measurements were performed during DAISEX'99 (*http://io.uv.es/projects/daisex/*), a campaign in the framework of the European Space Agency's Earth Observation Preparatory Programme [8]. From 1998 through 2000, this campaign was conducted on an agricultural test site in Spain (39°03′ N, 2°05′ W) to demonstrate the estimation of geo/biophysical variables from imaging spectrometer data. In 1999, the airborne sensors DAIS7915 [9], HYMAP (*http://www.intspec.com*), and POLDER [10] were flown at three times throughout the day. Simultaneous diurnal HDRF measurements of the Alfalfa canopy exhibit the effect of changing view and sun direction, whereas their high spectral resolution allows analyzing wavelength-dependent anisotropy effects.

A description of the experimental design, the preprocessing and quality analysis methodology is followed by the presentation of reflectance simulations. The PROSPECT model [11] is used to simulate leaf optical properties needed to calculate the reflectance of the canopy with the Scattering by Arbitrarily Inclined Leaves, with Hot spot effect (SAILH) model [12]. The statistical analysis of the observed data is a prerequisite to quantify the influence of directional effects on the vegetation variable estimation using empirical and semiempirical methodologies (e.g., vegetation indices) neglecting the anisotropy.

Spectrodirectional reflectance data of crops serve as input to radiative transfer models, coupled with canopy functioning models, applied in precision farming and yield prediction [13]. Thus, measured and simulated reflectances are compared quantitatively with the objective of predicting canopy structure variables, using vegetation models in inverse mode. Modeled reflectances serve as a reference to analyze directional observations' uncertainties and determine differences in their representation of spectrodirectional effects. A methodology for the normalization of measured HDRF data is presented, simplifying the analysis of wavelength dependence of the anisotropy of canopy reflectance.

II. Experimental Site and Instruments

A. Alfalfa Characteristics

The study concentrates on the bidirectional reflectance characterization of the agricultural crop Alfalfa, a mainstay in the production of livestock products, and recognized as the oldest plant grown solely for forage. The estimate of worldwide acreage amounted to 32 million ha in 1988. The worldwide importance of Alfalfa is attributed to its high yield of nutritious

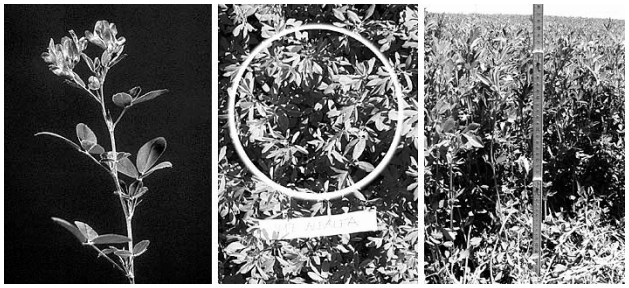

(a) (b) (c)

Fig. 1. (a) Alfalfa stem photograph (Copyright Oregon State University, Forage Information System). (b) Projected nadir ground instantaneous field of view of the GER3700 spectrometer onto the Alfalfa canopy [23]. (c) Side view of the observed canopy [23].

herbage, rapid recovery after cutting, longevity, and tolerance to environmental stress [14].

Alfalfa is a heliotropic plant, which means that architectural changes occur caused by the movement of the sun during the day [15]. Both diaheliotropic (i.e., leaf surface perpendicular to the direction of incident radiation) and paraheliotropic (leaf orientation parallel to incident radiation) movements are reported [16], [17].

The observed Alfalfa canopy was irrigated and dense, in the late bud stage (Fig. 1).[1] The height of the canopy was 50 cm, the fresh biomass 1880 g/m^2 and the leave's Dry Matter (DM) per ground area 22.3 mg/cm^2. Measurements performed using a Licor LAI 2000 instrument [18] indicated a leaf area index (LAI) of three. Calculating the specific leaf mass (SLM) from the given leave's dry matter and the LAI (SLM $=$ DM/LAI), an SLM of 7.4 mg/cm^2 results, a value which is considered too high compared to published ranges for Alfalfa at about the same maturity stage [19], [20]. LAI 2000 measurements taken under direct illumination conditions can result in an underestimation of LAI values, up to a factor 1.8 [18]. Thus, a true LAI could be between 3 and 5.5. The upper bound of the LAI variation is used in model calculations (see Section IV-B), leading to a more realistic SLM of 4 mg/cm^2. In the case of dense canopies ($LAI > 3$) its reflectance can be insensitive to LAI [21], [22]. Therefore, setting LAI value to 5.5 does not lead to a significant mistake in the modeled canopy reflectance.

B. Experimental Design of FIGOS Measurements

The FIGOS goniometer [7] is operated with a GER3700 having a field of view of 3° and a spectral range from 0.4–2.5 μm, calibrated for absolute radiance traceable to a NIST (National Institute of Standards and Technology, USA) calibration standard [24]. Mounted on the zenith arc of the goniometer, the footprint of the spectroradiometer has a radius of 5.2 cm at nadir position. In increments of 15° in zenith and 30° in azimuth direction, 66 target and seven Spectralon panel measurements covering a full hemisphere are recorded in about 23 min. The reference panel nadir view measurements allow for the derivation of the surface HDRF. A Reagan sunphotometer measuring the direct irradiance is set up next to FIGOS, enabling the simulation of the diffuse part of the total irradiance.

[1]http://forages.orst.edu/IS/NAIS/main.cfm?PageID=41

III. Methodology

A. Preprocessing of Measured Directional Reflectance Data

Following the reflectance nomenclature of Martonchik *et al.* [25], quantities measured with FIGOS correspond to the surface-leaving radiance reflected by the target L_r and the Spectralon panel L_r^{ref}. Due to the sensors ground instantaneous field of view (GIFOV) exceeding the area of the Spectralon for large view zenith angles, panel measurements are performed only from the nadir view direction.

To derive the hemispherical-directional reflectance factor (HDRF) R^{hem} for each view angle, the surface-leaving radiance is divided by the radiance from a Lambertian reflector illuminated under the same ambient conditions. Due to deviations from a perfectly Lambertian and lossless reflectance behavior of the Spectralon panel, a correction factor is introduced, which ideally corresponds to the bidirectional reflectance factor (BRF) R^{ref} of the panel. By introducing the actual sun zenith angle θ_i of the directional measurements in the following equation, the correction factor k is derived [26]:

$$k(\theta_i, \lambda) = a_0(\lambda) + a_1(\lambda)\theta_i + a_2(\lambda)\theta_i^2 \tag{1}$$

where θ_i is the solar zenith angle; λ is the wavelength; and a_0, a_1, and a_2 represent the coefficients for the polynomial fit of the Spectralon panel BRDF derived in a laboratory experiment [26]. For solar zenith angles of 17° to 53°, k varies from 0.89 to 0.926, respectively with minor differences among wavelengths. Thus, the HDRF (R^{hem}) calculation from field measurements results in the following formula:

$$R^{\mathrm{hem}}(\theta_i, \phi_i, \theta_r, \phi_r, \lambda) = \frac{L_r(\theta_i, \phi_i, \theta_r, \phi_r, \lambda)}{L_r^{\mathrm{ref}}(\theta_i, \phi_i, \theta_r = 0, \phi_r = 0, \lambda)} \times k(\theta_i, \lambda) \tag{2}$$

whereas θ_i, ϕ_i, θ_r, and ϕ_r are the zenith and azimuth angles of the direction of illumination and reflection, respectively.

Due to self-shadowing of the target by the sensor in the hot spot direction for view angles located 10° around the actual sun zenith angle, corresponding HDRF data in the solar principle plane cannot be measured with FIGOS. Wavelength regions with sensor artifacts (cf., [24]) and low atmospheric transmittance ($< 20\%$) are excluded from further analysis. Gaseous transmittance was derived from forward simulations using MODTRAN4 [27] with atmospheric conditions derived from inverted sunphotometer data acquired simultaneously with the FIGOS measurements and the spectral response function of the GER3700 spectrometer.

In the following, single view angle FIGOS observations will be referred to as "measurements," whereas a FIGOS hemisphere includes reflectances of a full scan of the view hemisphere (i.e., 66 measurements from different view angles for a single sun angle configuration).

The spectral albedo (BHR) A_{BHR} is computed to characterize the radiation budget over the whole hemisphere. The bihemispherical reflectance (A_{BHR}) is the ratio of the flux Φ_r of light reflected from surface area dS to the incident flux Φ_i [25]

$$A_{\mathrm{BHR}}(\lambda) = \frac{d\Phi_r(\lambda)}{d\Phi_i(\lambda)} = \frac{dS \int_{2\pi} L_r(\theta_r, \phi_r, \lambda) \cos\theta_r \sin\theta_r d\theta_r d\phi_r}{dS \int_{2\pi} L_i(\theta_i, \phi_i, \lambda) \cos\theta_i \sin\theta_i d\theta_i d\phi_i}. \tag{3}$$

During the DAISEX'99 experiment the irradiance Φ_i, required for the calculation of A_{BHR} using (3), was not observed, and therefore A_{BHR} is derived by integrating the HDRF data over all directions of the view hemisphere [26]

$$A_{\mathrm{BHR}}(\theta_i, \phi_i, \lambda) \approx \frac{1}{\pi} \cdot \int_0^{2\pi} \int_0^{\pi/2} R^{\mathrm{hem}}(\theta_i, \phi_i, \theta_r, \phi_r, \lambda) \cos\theta_r \sin\theta_r d\theta_r d\phi_r. \quad (4)$$

B. Quality Assessment: Sources of Uncertainties of Measured HDRF

The observed surface's BRDF and experimental artifacts, reducing the additional information content of multiangular data, cause the variation of HDRF field measurements. Therefore the quantification of uncertainties of the HDRF introduced by sources as discussed in the following paragraphs is a prerequisite for further analysis of the data.

1) Sensor Uncertainties: FIGOS deploys a radiance-calibrated GER3700 spectroradiometer, with determined detector specific uncertainties for reflectance measurements (i.e., $\pm 2.9\%$ to $\pm 6.16\%$ with a 10% changing atmosphere between reference and target measurement) [24].

2) Panel Correction Uncertainties: As described in Section III-A, the HDRF calculation includes a Spectralon panel correction with a polynomial fit representing its BRF where angles have not been measured. The root mean square error of the fit with regard to the measured BRF varied from 1.4% to 2.2% reflectance for the wavelength range 0.45–1.0 μm.

3) Not Quantified Additional Sources of Variation: Even though the sun's geometry is changing during the time of the 66 target measurements of a hemisphere (see Section II-B), it is assumed to be constant. Maximum values for the change of the azimuth were reached around noon (up to 20°), whereas in the morning and evening the deviations of the azimuth decreased and the zenith angle changes reached up to 6°.

Due to the constant focal length of the GER3700 optics, the extent of the GIFOV changes with the view zenith angle according to the cosine projection law. For nadir measurements, the ellipse of the sensor's footprint has a length of 10 cm and increases to 40 cm for a view angle of 75°. Thus, inhomogeneity of the target introduces additional uncertainties.

A still poorly understood effect of the BRDF is its scale dependence. For the characterization of the Alfalfa canopy BRDF, the scattering elements (i.e., the individual leaves) could be at a critical size with respect to the limited GIFOV of FIGOS.

Throughout the day, changes in vegetation structural properties (e.g., leaf angle distribution [16]) due to physiological and biochemical variations of the plants may cause variations of the measured directional reflectance. Due to missing information about the vegetation properties throughout the day it is not possible to quantify this part of the variation.

C. Vegetation Canopy HDRF Simulations

To establish a reference for the measured Alfalfa HDRF data, leaf optical properties and canopy reflectance were calculated using PROSPECT [11] and SAILH [12]. Vegetation and actual atmospheric conditions as well as soil reflectance measured on the test site served as model input.

D. Statistical Analysis

To assess the range of variation of HDRF data due to the changing view and sun direction throughout the day, a statistical analysis of measured and modeled HDRFs is performed, with a special emphasis on the wavelength specific behavior. The results reveal the variation of directional data corresponding to structural information about the vegetation canopy, compared to the data uncertainties introduced by artifacts mentioned in Section III-B.

The first analysis includes the overall variation of all preprocessed HDRFs, i.e., the calculation of the mean, standard deviation, and coefficient of variation (standard deviation divided by mean) over all view and sun directions. Thereafter, the variation of the HDRFs of each hemisphere is calculated, showing the information content of all view angles for an approximately constant solar position. A third analysis demonstrates the deviation of nadir view measurements acquired at different sun zenith angles from the nadir view spectrum around solar noon (i.e., solar zenith angle of 17°). The difference of the noon spectrum minus the actual spectrum is divided by the noon spectrum to obtain the normalized deviation.

E. Analysis of Wavelength Dependence

Vegetation canopy HDRF data exhibit pronounced wavelength-dependent effects, which can be described by anisotropy factors [28]. In order to derive the relative deviation of each view angle reflectance, measured HDRF data are divided by a standard target spectrum. In this study the calculated bihemispherical reflectance of each observed hemisphere is chosen as standard spectrum instead of the usually applied nadir reflectance [26], [28]. The anisotropy factor $\mathrm{ANIF}_{\mathrm{BHR}}$ refers to the deviation of the reflection behavior in a specific view direction from the BHR, for the actual irradiance conditions of the measured hemisphere

$$\mathrm{ANIF}_{\mathrm{BHR}}(\theta_i, \phi_i, \theta_r, \phi_r, \lambda) = \frac{R^{\mathrm{hem}}(\theta_i, \phi_i, \theta_r, \phi_r, \lambda)}{A_{\mathrm{BHR}}(\theta_i, \phi_i, \lambda)}. \quad (5)$$

IV. Observed Spectrodirectional Data and Model Simulations

A. Preprocessing and Resulting Alfalfa HDRF Data

Measured directional reflectance is converted to HDRF data as in Section III-A, accounting for the non-Lambertian and absorbing behavior of the Spectralon panel, shaded target measurements, and wavelength ranges with sensor artifacts and low atmospheric transmittance. Low total gaseous transmittance wavelength ranges were identified at 1.3 μm and 1.8–1.9 μm. The preprocessing resulted in eight hemispheres of Alfalfa HDRF data used for further analysis (Table I).

B. PROSPECT/SAILH Simulation Description

Using the modeling approach as defined in Section III-C, the input parameters for PROSPECT and SAILH are determined.

TABLE I
HDRF HEMISPHERES OF THE ALFALFA CANOPY AFTER PREPROCESSING (sa = AVERAGE SUN AZIMUTH RELATIVE TO GEOGRAPHIC NORTH, sz = AVERAGE SUN ZENITH ANGLE, no. M. = NUMBER OF REFLECTANCE MEASUREMENTS PER HEMISPHERE AFTER PROCESSING)

Hemisphere	sa [°]	sz [°]	no. m.	Hemisphere	sa [°]	sz [°]	no. m.
1	90.0	53.0	59	5	224.5	22.0	63
2	107.0	35.8	64	6	246.5	31.3	66
3	140.8	20.5	64	7	254.8	37.3	66
4	181.5	17.0	66	8	262.5	44.8	66

TABLE II
SAILH INPUT PARAMETERS USED FOR SIMULATION RUNS OF ALFALFA HDRF FOR ALL VIEW AND SUN ANGLES OF THE DAY

SAILH parameter	**Input value**		**SAILH parameter**	**Input value**	
Leaf area index	5.5	Constant	Soil reflectance	Nadir reflectance measured at test site	Constant
Average leaf angle	50°	Constant	View zenith angle	Angular position of FIGOS	Variable
Hot spot parameter	0.057	Constant	Sun zenith angle	Corresponding to mean solar angle of individual FIGOS hemispheres	Variable
Leaf reflectance	PROSPECT output	Constant	Relative azimuth Sun-sensor	Angular position of FIGOS	Variable
Leaf transmittance	PROSPECT output	Constant	Diffuse fraction	From MODTRAN4	Variable

An average leaf angle of the Alfalfa canopy and the leaf structure parameter N [11] are derived from the literature [6]. The LAI is used to calculate the leaf chlorophyll, and leaf water from observed canopy amounts (see Section II-A). A PROSPECT run for the identified leaf biochemical and structural characteristics (structure parameter $N = 1.8$, chlorophyll a and b content $C_{ab} = 41.4\ \mu\text{g/cm}^2$, equivalent water thickness $C_w = 0.022$ cm, dry matter content $C_m = 0.004\ \text{g/cm}^2$, brown pigment content $= 0.1$) is performed. The resulting leaf reflectance and transmittance serve as input to SAILH, together with the canopy architecture characteristics, the observed soil reflectance, and the ratio of diffuse to total irradiance. The latter was derived from sunphotometer data for each FIGOS hemisphere using the optical depth from the sunphotometer as input to MODTRAN4 [27]. The resulting ratio for the actual conditions is wavelength (between 0.26 and 0.36 at 0.4 μm and decreasing to 0.05 at 0.8 μm) and time dependent, with a minimum around solar noon.

Finally, a run of SAILH for the geometry of each goniometer measurement is performed (Table II). Resulting HDRF data are resampled to the spectral resolution of the preprocessed FIGOS measurements.

V. RESULTS

A. Resulting HDRF Data and Their Quality

1) Statistical Analysis: Calculated mean values of measured and modeled Alfalfa HDRF data over all view and sun directions show similar shapes, especially in the visible wavelength region (Fig. 2). The standard deviation and coefficient of variation of the measured HDRF are wavelength dependent. The mean variation over all wavelengths amounts to 17.7% and therefore is larger than the mean variation of the modeled HDRF data (11.1%).

Wavelength regions with low mean reflectance (e.g., the red spectral region around 680 nm) exhibit a larger variation in HDRF data, compared to high reflectance values with a rather small variation (e.g., the NIR region). This behavior of the HDRF data cannot be explained as an instrumental artifact, because modeled data show the same tendency. The explanation is found in the decreased anisotropy for wavelength regions with high reflectance and therefore a higher amount of multiple scattering. These findings are consistent with a study describing the anisotropy of an Alfalfa canopy in the red and NIR spectral region assessing the influence of sun and sensor geometry on the normalized difference vegetation index and the soil adjusted vegetation index [5].

The analysis of the mean HDRF data and their variation with respect to diurnal dynamics shows that the range of variation of the different view angles is related to the sun zenith angle (Fig. 3). HDRFs exhibit a larger variation for large sun zenith angles, i.e., a more pronounced directional behavior than HDRF data acquired around solar noon.

2) Nadir Alfalfa HDRF Variations Throughout the Day: Field spectrometer measurements serve as a reference for air- and spaceborne remote sensing data and are used for vicarious calibration purposes. Therefore they are optimally acquired simultaneously to the overflight. The following analysis derives the deviations of the diurnal nadir Alfalfa HDRFs from a perfectly timed measurement.

The differences between the nadir view HDRF around solar noon (sun zenith angle of 17°) and nadir view HDRFs measured at different sun zenith angles throughout the day, normalized by the solar noon HDRF are shown in Fig. 4. The relative HDRF deviations are wavelength dependent and considerably larger for wavelength regions with low reflectance values (e.g., red spectral bands around 0.6 μm) compared to spectral regions with high canopy reflectance (e.g., NIR). In the visible

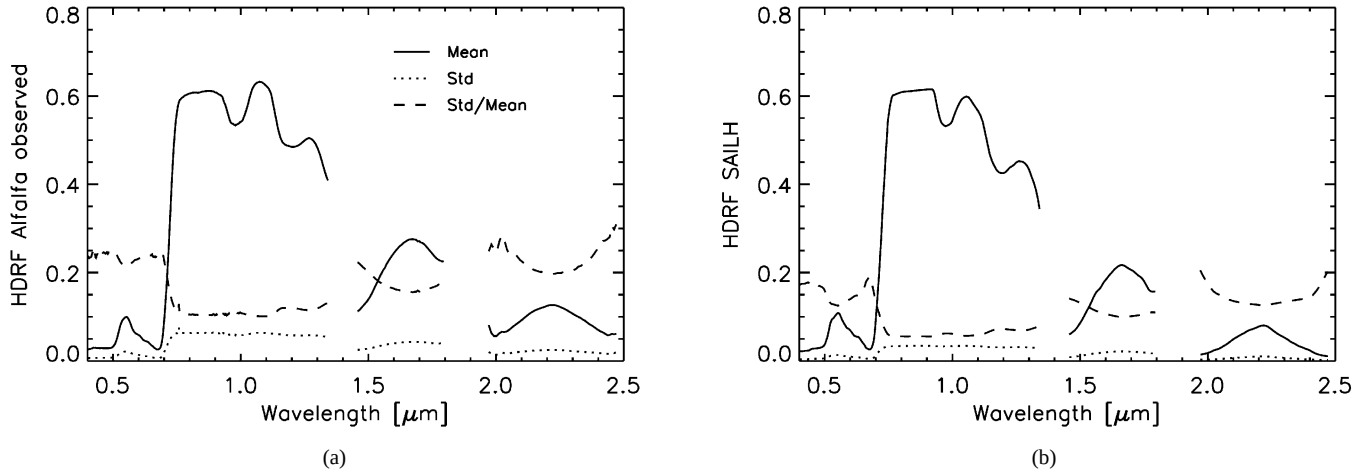

(a) (b)

Fig. 2. Overall statistics for (a) measured and (b) simulated Alfalfa HDRF data over all sun and view directions.

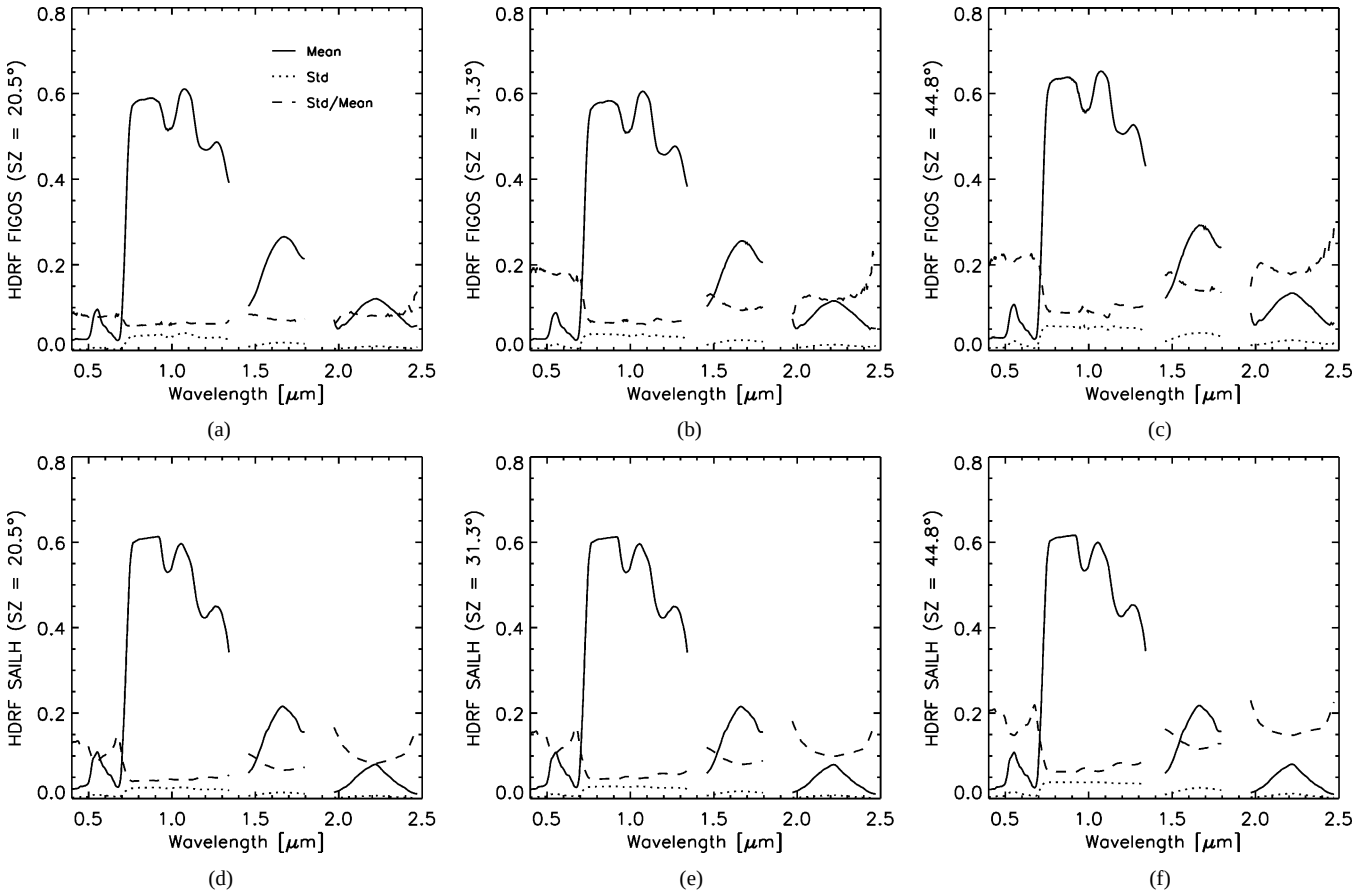

(a) (b) (c)

(d) (e) (f)

Fig. 3. (a)–(c) Statistics for measured and (d)–(f) simulated Alfalfa HDRF data of the whole hemisphere for three sun zenith angles throughout the day.

part of the spectrum HDRF data are up to 40% below solar noon measurements. The deviations in measured data result from the changing sun direction, atmospheric and vegetation conditions as well as spectroradiometer uncertainties. Even though simulations account for changing sun angles and atmospheric conditions, modeled HDRF deviations are much smaller and within 20% of the reference noon reflectance. Further, measured data do not follow the trend of simulations, where absolute deviations increase with increasing solar zenith angle. Nadir observations are biggest for illumination geometries corresponding to solar noon and early morning, thus lying in the hot spot area, and exhibit the lowest reflectances for solar zenith angles around 36°. The difference between simulated and measured data could be found in the changes of vegetation structure throughout the day, which was neither assessed in the field nor taken into account in the simulations. The analysis illustrate the need of measurements at the exact time of the overflight for vicarious calibration purposes of imaging spectrometer data and the necessity of taking into account the sun angle geometries for field spectrometer measurements.

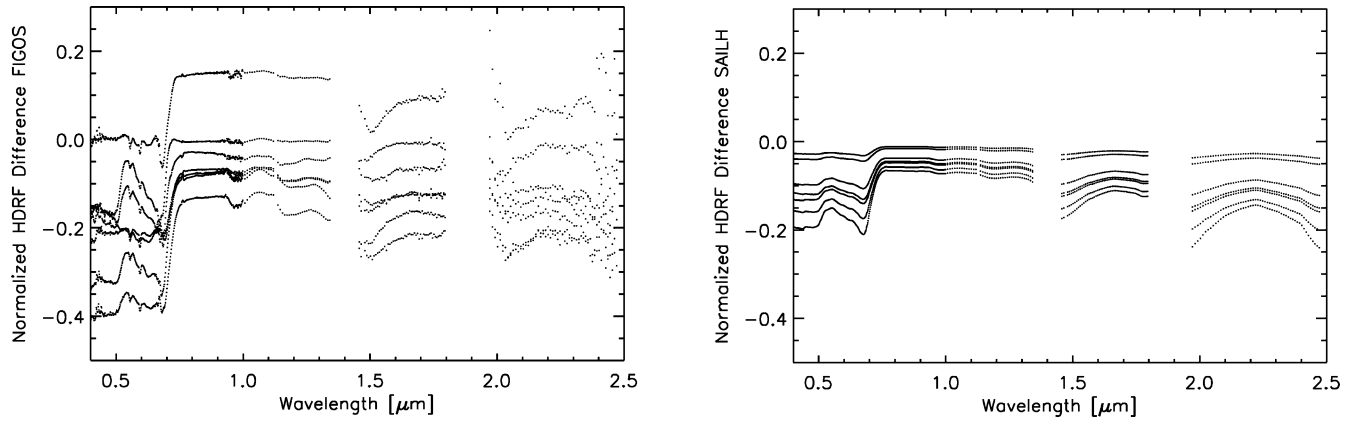

(a) (b)

Fig. 4. (a) Deviations of nadir view HDRF measurements [HDRF difference for solar zenith angles of 53.0°, 20.5°, 44.8°, 31.3°, 22.0°, 35.8°, and 37.3° (from top to bottom)] and (b) simulations [HDRF difference for solar zenith angles of 20.5°, 22.0°, 31.3°, 35.8°, 37.3°, 44.8°, and 53.0° (from top to bottom)] of the Alfalfa canopy from corresponding HDRF around solar noon (i.e., nadir view HDRF for solar zenith angle of 17.0°), normalized by the solar noon HDRF.

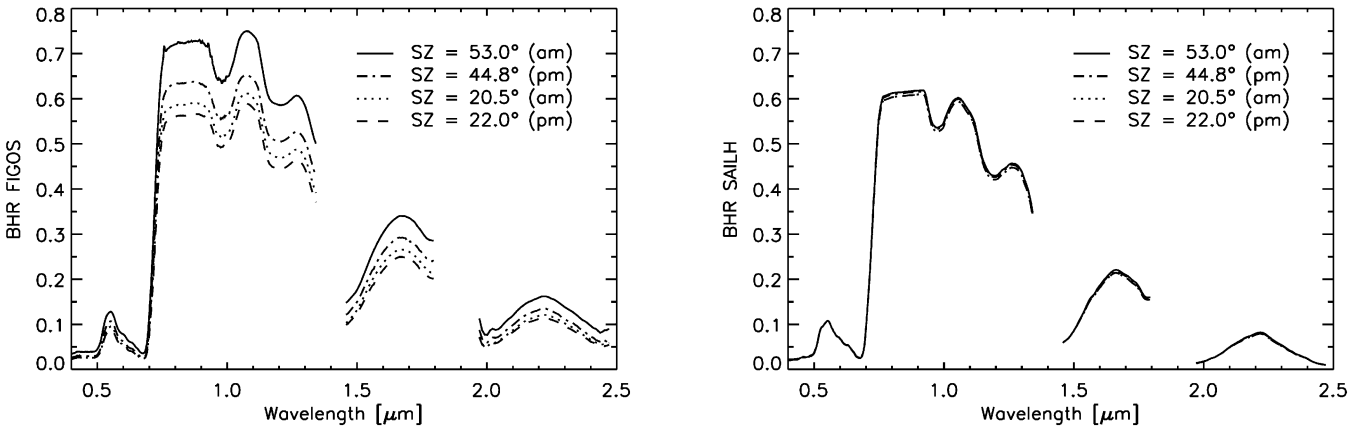

(a) (b)

Fig. 5. BHR results of the dense Alfalfa canopy for different solar angles throughout the day derived from (a) measured and (b) simulated HDRF data. Note the higher albedo for the morning solar zenith angle of 20.5° compared to the lower albedo of the afternoon albedo at a solar zenith of 22.0°.

B. BHR Results

The calculated BHR for measured and simulated Alfalfa canopy hemispheres basically increases with growing sun zenith angle (Fig. 5), in accordance with albedo trends reported in other studies [29]–[31]. The average variation of the BHR derived from measured data reaches 12.7% over all wavelengths, whereas simulated data varies only by 1%, even though changes of the sun position and atmospheric conditions are accounted for in the simulations.

The albedo basically is an increasing function of the solar zenith angle, but shows an asymmetric behavior with regard to solar noon [29]. Analyzing morning and afternoon spectral albedos derived from measurements (Fig. 5), the BHR averaged over the measured wavelength range is considerably larger for morning conditions (e.g., solar zenith angle of 20.5°) than the corresponding afternoon albedo (e.g., solar zenith angle of 22.0°).

Large solar zenith angles evoke a more pronounced variation of the HDRF over the whole view angle hemisphere compared to sun positions around noon (Fig. 3). HDRF data were related to the corresponding BHR to analyze their spectral behavior (Fig. 6). SAILH simulated HDRF variations are large for wavelengths with a low BHR. In highly reflecting spectral regions the anisotropy is much less pronounced in terms of variation of the HDRF, most likely due to multiple scattering effects smoothing directional effects. Comparing measured HDRF data to the BHR, the above-mentioned relation exists for large solar zenith angles, whereas small solar zenith angles show a less pronounced anisotropy (Fig. 6). The variation of the HDRF measured at a solar zenith of 20.5° amounts to 6 to 10% for most wavelength regions, being almost constant with regard to the actual canopy BHR. The various variation levels for different wavelengths with the same BHR exposed in measured data indicate that anisotropy effects not correlated to the spectral albedo do exist.

C. Results From Normalization Procedure

Normalizing HDRF data with the corresponding BHR emphasizes wavelength dependence of the anisotropy. Anisotropy factors, $\mathrm{ANIF}_{\mathrm{BHR}}$ [see (5)], derived from SAILH nadir view simulations show a very similar wavelength-dependent behavior for different sun zenith angles, i.e., mainly an offset of the anisotropy factors for the three different times of the day, with higher values for highly absorbing wavelength regions

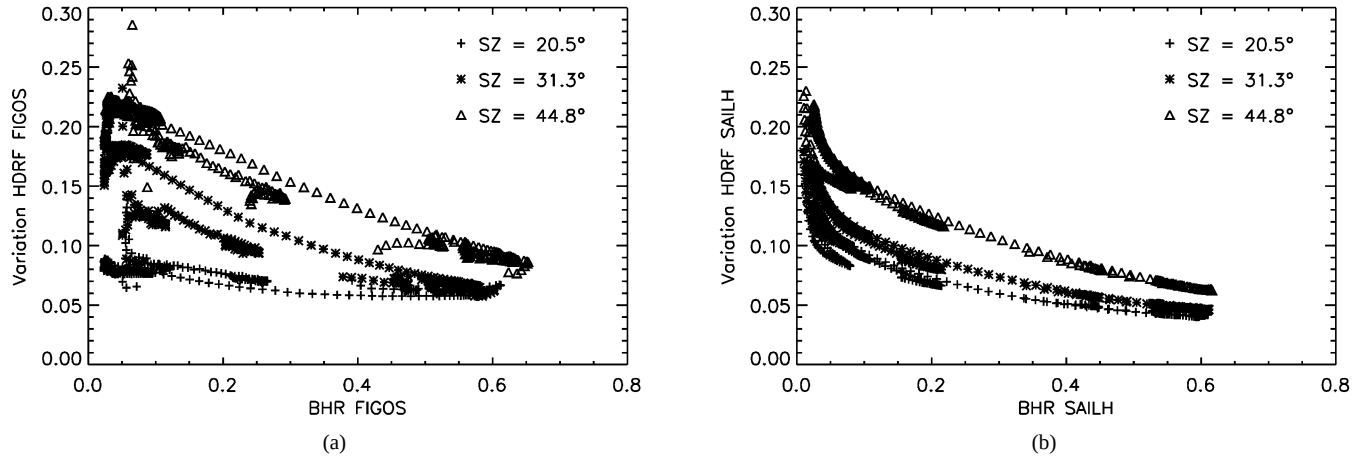

(a) (b)

Fig. 6. Variation of HDRF versus BHR for each wavelength of (a) measured and (b) simulated Alfalfa canopy data for three solar zenith angles.

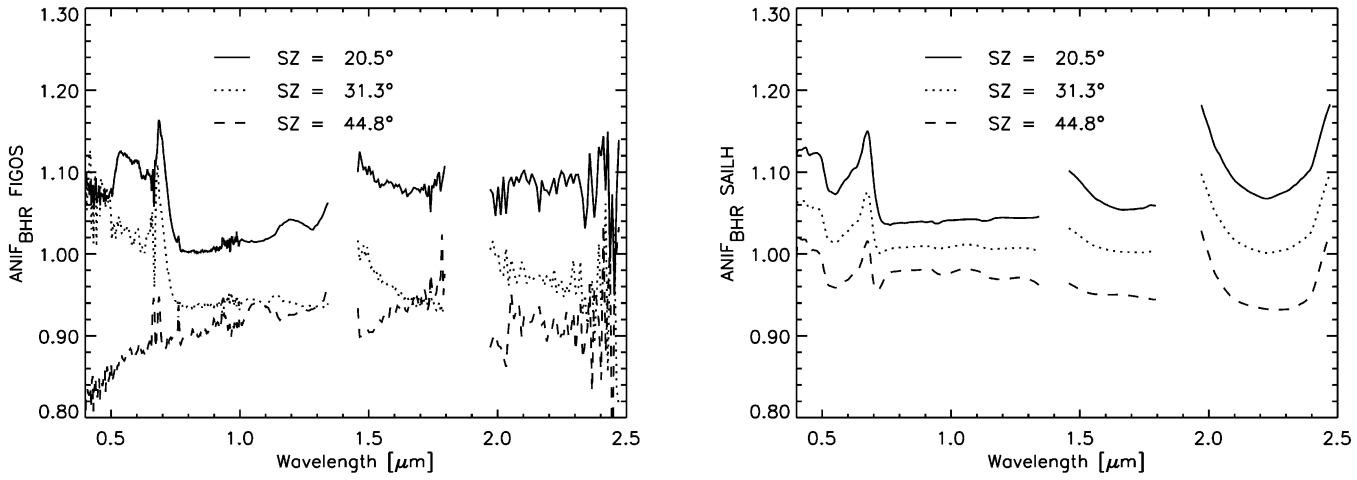

(a) (b)

Fig. 7. $\mathrm{ANIF_{BHR}}$ from (a) FIGOS measurements and (b) SAILH simulations for the nadir view angle at three different sun zenith angles of the day.

(Fig. 7). $\mathrm{ANIF_{BHR}}$ derived from measured data exhibit a more complex shape, especially in the visible spectral range.

VI. Conclusion

This study suggests a standard procedure to analyze field goniometer data for their quality and quantify their information content with regard to observations' uncertainties. The preprocessing includes the derivation of HDRFs from measured radiances, taking into account the deviations of the Spectralon panel from a perfect Lambertian reflector, as well as system and atmosphere properties. An overall characterization of the target's spectral anisotropy is performed using statistical analysis, the spectral albedo, BHR, and the anisotropy factor $\mathrm{ANIF_{BHR}}$. The comparison of modeled and observed data is a tool to assess differences in their representation of spectrodirectional effects and assign corresponding uncertainties to HDRF data.

Nadir HDRF measurements throughout the day exhibit large deviations due to a changing solar position and canopy architecture, whereas simulations show smaller deviations. Thus, the HDRF should be measured in field experiments and vicarious calibration procedures at the time it is needed, rather than simulated. The results on the BHR substantiate previous studies: the albedo increases with growing sun zenith angle, and an asymmetry with respect to solar noon exists.

The presented procedure guarantees the quality and uncertainty assessment required for the use of spectrodirectional reflectance available in *a priori* BRDF knowledge databases. Even though observed and modeled Alfalfa canopy data show similar trends for the overall statistical analysis, spectral effects are not fully reproduced by simulations.

Future analyses of the spectral effects in the anisotropy of vegetation reflectance require simultaneous measurements of the canopy transmittance and leaf optical properties. They will allow to verify more complex algorithms for estimating vegetation variables, which are based on theories explaining the canopy reflectance in the solar reflected spectral region using leaf optical properties in combination with wavelength-independent variables, characterizing the architecture of the canopy [12], [32]. Laboratory measurements with joint outdoor observations are planned to separate the illumination components for deriving BRFs and the BRDF and eliminating spectral effects introduced by the atmosphere, and thus enabling investigations on the separated vegetation-dependent spectral effects of the canopy anisotropy.

ACKNOWLEDGMENT

The authors would like to thank the DAISEX field team, J. Moreno (University of Valencia), W. Verhoef (National Aerospace Center), J. Keller (Paul Scherrer Institut), S. Dangel, U. Beisl, and C. Dickerhof for their support and fruitful discussions. The authors thank the reviewers for helpful comments on the manuscript, allowing for substantial improvements.

REFERENCES

[1] W. A. Abdou, J. E. Conel, S. H. Pilorz, M. C. Helmlinger, C. J. Bruegge, B. J. Gaitley, W. C. Ledeboer, and J. V. Martonchik, "Vicarious calibration. A reflectance-based experiment with AirMISR," *Remote Sens. Environ.*, vol. 77, pp. 338–353, 2001.

[2] U. Beisl, "Correction of bidirectional effects in imaging spectrometer data," in *Remote Sensing Series*. Zürich, Switzerland: RSL, 2001, vol. 37, p. 189.

[3] X. Li, F. Gao, J. Wang, and A. Strahler, "A priori knowledge accumulation and its application to linear BRDF model inversion," *J. Geophys. Res.*, vol. 106, no. 11, pp. 11 925–11 935, 2001.

[4] M. E. Bauer, C. Daughtry, L. Biehl, E. Kanemasu, and F. Hall, "Field spectroscopy of agricultural crops," *IEEE Trans. Geosci. Remote Sensing*, vol. GE-24, pp. 65–75, Jan. 1986.

[5] J. C. Epiphanio and A. R. Huete, "Dependence of NDVI and SAVI on sun/sensor geometry and its effect on FAPAR relationships in Alfalfa," *Remote Sens. Environ.*, vol. 51, pp. 351–360, 1995.

[6] A. Walter-Shea, J. Privette, D. Cornell, M. A. Mesarch, and C. J. Hays, "Relations between directional spectral vegetation indices and leaf area and absorbed radiation in Alfalfa," *Remote Sens. Environ.*, vol. 61, pp. 162–177, 1997.

[7] S. R. Sandmeier and K. I. Itten, "A field goniometer system (FIGOS) for acquisition of hyperspectral BRDF data," *IEEE Trans. Geosci. Remote Sensing*, vol. 37, pp. 978–986, Mar. 1999.

[8] M. Berger, M. Rast, P. Wursteisen, E. Attema, J. Moreno, A. Mueller, U. Beisl, R. Richter, M. Schaepman, G. Strub, M. P. Stoll, F. Nerry, and M. E. Leroy, "The DAISEX campaigns in support of a future land-surface-processes mission," *ESA Bull.*, vol. 105, pp. 101–111, 2001.

[9] S. H. Chang, M. J. Westfield, F. Lehmann, D. Oertel, and R. Richter, "79- channel airborne imaging spectrometer," in *SPIE*, vol. 1937, 1993, pp. 164–172.

[10] J. L. Deuze, F. M. Breon, J. C. Roujean, P. Y. Deschamps, C. Devaux, M. Herman, and A. Podaire, "Analysis of the POLDER (POLarization and directionality of earth's reflectances) airborne instrument observations over land surfaces," *Remote Sens. Environ.*, vol. 45, pp. 137–154, 1994.

[11] S. Jacquemoud and F. Baret, "PROSPECT: A model of leaf optical properties spectra," *Remote Sens. Environ.*, vol. 34, pp. 75–91, 1990.

[12] W. Verhoef, "Theory of radiative transfer models applied in optical remote sensing of vegetation canopies," Ph.D. thesis, National Aerospace Lab., Amsterdam, The Netherlands, 1998.

[13] M. Weiss, D. Troufleau, F. Baret, H. Chauki, L. Prevot, A. Olioso, N. Bruguier, and N. Brisson, "Coupling canopy functioning and radiative transfer models for remote sensing data assimilation," *Remote Sens. Environ.*, vol. 108, pp. 113–128, 2001.

[14] A. A. Hanson, D. K. Barnes, and R. R. Hill, Eds., "Alfalfa and Alfalfa improvement," in *Agronomy*. Madison, WI: Amer. Soc. Agronomy, 1988, p. 1084.

[15] J. R. Ehleringer and I. N. Forseth, "Solar tracking by plants," *Science*, vol. 210, pp. 1094–1098, 1980.

[16] R. L. Travis and R. Reed, "The solar tracking pattern in a closed Alfalfa canopy," *Crop Sci.*, vol. 23, pp. 664–668, 1983.

[17] M. S. Moran, P. J. Pinter, B. E. Clothier, and G. A. Stephen, "Effect of water stress on the canopy architecture and spectral indices of irrigated Alfalfa," *Remote Sens. Environ.*, vol. 29, no. 3, pp. 251–261, 1989.

[18] J. M. Welles and J. M. Norman, "Instrument for indirect measurement of canopy architecture," *Agronomy J.*, vol. 83, no. 5, pp. 818–825, 1991.

[19] I. M. Ray, M. S. Townsend, and J. A. Henning, "Variation for yield, water-use efficiency, and canopy morphology among nine Alfalfa germplasms," *Crop Sci.*, vol. 38, pp. 1386–1390, 1998.

[20] R. H. Hart, R. B. Pearce, N. J. Chatterton, G. E. Carlson, D. K. Barnes, and C. H. Hanson, "Alfalfa yield, specific leaf weight, CO_2 exchange rate, and morphology," *Crop Sci.*, vol. 18, pp. 649–653, 1978.

[21] N. Gobron, B. Pinty, M. Verstraete, and Y. Govaerts, "A semidiscrete model for the scattering of light by vegetation," *J. Geophys. Res.*, vol. 102, no. 8, pp. 9431–9446, 1997.

[22] Y. Knyazikhin, J. V. Martonchik, D. J. Diner, R. B. Myneni, M. Verstraete, B. Pinty, and N. Gobron, "Estimation of vegetation canopy leaf area index and fraction of absorbed photosynthetically active radiation from atmosphere-corrected MISR data," *J. Geophys. Res.*, vol. 103, no. 24, pp. 32 239–32 256, 1998.

[23] J. Moreno *et al.*, "DAISEX-1999 field experiment report," Univ. Valencia, Valencia, Spain, ESA/ESTEC Contract 13 390/NL/GD, 1999.

[24] M. E. Schaepman and S. Dangel, "Solid laboratory calibration of a nonimaging spectroradiometer," *Appl. Opt.*, vol. 39, no. 1, pp. 3754–3764, 2000.

[25] J. V. Martonchik, C. J. Bruegge, and A. H. Strahler, "A review of reflectance nomenclature used in remote sensing," *Remote Sens. Rev.*, vol. 19, pp. 9–20, 2000.

[26] S. Sandmeier, C. Müller, B. Hosgood, and G. Andreoli, "Sensitivity analysis and quality assessment of laboratory BRDF data," *Remote Sens. Environ.*, vol. 64, pp. 176–191, 1998.

[27] A. Berk, G. Anderson, L. Bernstein, P. Acharya, H. Dothe, M. Matthew, S. Adler-Golden, J. Chetwynd, and S. Richtsmeier, "MODTRAN 4 radiative transfer modeling for atmospheric correction," in *Proc. 8th JPL Airborne Earth Science Workshop*, Pasadena, CA, 1999, pp. 55–61.

[28] S. R. Sandmeier, E. M. Middleton, D. W. Deering, and W. Qin, "The potential of hyperspectral bidirectional reflectance distribution function data for grass canopy characterization," *J. Geophys. Res.*, vol. 104, no. 8, pp. 9547–9560, 1999.

[29] P. Minnis, S. Mayor, W. L. Smith, and D. F. Young, "Asymmetry in the diurnal variation of surface albedo," *IEEE Trans. Geosci. Remote Sensing*, vol. 35, pp. 879–891, July 1997.

[30] W. Lucht, C. B. Schaaf, and A. H. Strahler, "An algorithm for the retrieval of albedo from space using semiempirical BRDF models," *IEEE Trans. Geosci. Remote Sensing*, vol. 38, pp. 977–998, Mar. 2000.

[31] S. Liang, J. C. Stroeve, I. F. Grant, A. H. Strahler, and J. P. Duvel, "Angular corrections to satellite data for estimating earth radiation budget," *Remote Sensing Rev.*, vol. 18, no. 24, pp. 103–136, 2000.

[32] O. Panferov, Y. Knyazikhin, R. B. Myneni, J. Szarzynski, S. Engwald, K. G. Schnitzler, and G. Gravenhorst, "The role of canopy structure in the spectral variation of transmission and absorption of solar radiation in vegetation canopies," *IEEE Trans. Geosci. Remote Sensing*, vol. 39, pp. 241–253, Feb. 2001.

Gabriela Strub received the M.S. degree in geography from the University of Zurich, Zurich, Switzerland, in 1999. She is currently pursuing the Ph.D. degree at the University of Zurich.

She is currently a Research Assistant with the Remote Sensing Laboratories, Department of Geography, University of Zurich, Switzerland since 1999. In 2001, she was a Research Scholar at the Department of Geography, Boston University, Boston, MA. Her research interests include analysis of spectrodirectional remote sensing data and variable estimation of vegetation canopies in support of precision farming and climate change related applications.

Michael E. Schaepman received the M.S. degree in geography and the Ph.D. degree (Dr. Sc. Nat.) in remote sensing, with emphasis on spectroscopy and calibration, from the University of Zurich, Zurich, Switzerland, in 1993 and 1998, respectively.

He is currently the Head of the Spectroscopy Laboratory of the Remote Sensing Laboratories, University of Zurich. In 1998, he has coinitiated the setup of an airborne imaging spectrometer named APEX, which is right now under construction with an international team of five industries and three institutions. He has worked as a Postdoc in the Optical Science Center, University of Arizona, Tucson, in 1999, and has since become Project Manager and Experiment Scientist for APEX. He is a founding member and Vice President of the board of Netcetera AG, Zurich, Switzerland, a software development company. His current research interest is in spectrodirectional imaging, design of dispersive pushbroom imaging spectrometers, and large volume data processing.

Dr. Schaepman is member of one Europeans Space Agency Core Mission Advisory Group, SPIE, OSA, and co-convenor of the EARSeL special interest group on imaging spectroscopy.

Yuri Knyazikhin received the M.S. degree in applied mathematics from Tartu University, Tartu, Estonia, and the Ph.D. degree in numerical analysis from the N.I. Muskhelishvilli Institute of Computing Mathematics, the Georgian Academy of Sciences, Tbilisi, Georgia, in 1978 and 1985, respectively.

He is currently a Research Professor in the Department of Geography, Boston University, MA. He was a Research Scientist at the Institute of Astrophysics and Atmospheric Physics, Tõravere, Estonia, as well as the Computer Center of the Siberian Branch of the Russian Academy of Sciences, Tartu University, from 1978 to 1990. He was an Alexander von Humboldt Fellow from 1992 to 1993, and worked at the University of Göttingen, Germany, from 1990 to 1996. He has worked and published in areas of numerical integral and differential equations, theory of radiation transfer in atmospheres and plant canopies, remote sensing of the atmosphere and plant canopies, ground-based radiation measurements, forest ecosystem dynamics, and modeling sustainable multifunctional forest management.

Klaus I. Itten (M'82–SM'97) received the M.S. and Ph.D. degrees in geography from the University of Zurich, Zurich, Switzerland, in 1969 and 1973.

He is currently a Professor in geography and remote sensing at the University of Zurich. As head of the Remote Sensing Laboratories at the University of Zurich, his research and teaching interests are remote sensing and image processing for natural resources inventorying and monitoring. In particular, the application of optical remote sensing, high spatial and spectral resolution image data, and analysis are the focus of his research. Imaging spectroscopy and spectroradiometry have become important parts of his endeavors.